archive ouverte UNIGE
http://archive-ouverte.unige.ch

Article

Optical Spin-Wave Storage in a Solid-State Hybridized Electron-Nuclear Spin Ensemble

BUSINGER, Moritz, *et al*.

Abstract

Solid-state impurity spins with optical control are currently investigated for quantum networks and repeaters. Among these, rare-earth-ion doped crystals are promising as quantum memories for light, with potentially long storage time, high multimode capacity, and high bandwidth. However, with spins there is often a tradeoff between bandwidth, which favors electronic spin, and memory time, which favors nuclear spins. Here, we present optical storage experiments using highly hybridized electron-nuclear hyperfine states in 171Yb3þ:Y2SiO5, where the hybridization can potentially offer both long storage time and high bandwidth. We reach a storage time of 1.2 ms and an optical storage bandwidth of 10 MHz that is currently only limited by the Rabi frequency of the optical control pulses. The memory efficiency in this proof-of-principle demonstration was about 3%. The experiment constitutes the first optical storage using spin states in any rareearth ion with electronic spin. These results pave the way for rare-earth based quantum memories with high bandwidth, long storage time, and high multimode capacity, a key resource for [...]

Reference

BUSINGER, Moritz, *et al*. Optical Spin-Wave Storage in a Solid-State Hybridized Electron-Nuclear Spin Ensemble. *Physical Review Letters*, 2020, vol. 124, no. 053606

DOI : 10.1103/PhysRevLett.124.053606

Available at:
http://archive-ouverte.unige.ch/unige:132184

Disclaimer: layout of this document may differ from the published version.

UNIVERSITÉ DE GENÈVE

Optical Spin-Wave Storage in a Solid-State Hybridized Electron-Nuclear Spin Ensemble

M. Businger,[1] A. Tiranov,[1,†] K. T. Kaczmarek,[1] S. Welinski,[2,‡] Z. Zhang,[2]
A. Ferrier,[2,3] P. Goldner,[2] and M. Afzelius[1,*]
[1]*Department of Applied Physics, University of Geneva, CH-1211 Genève, Switzerland*
[2]*Chimie ParisTech, PSL University, CNRS, Institut de Recherche de Chimie Paris, 75005 Paris, France*
[3]*Faculté des Sciences et Ingnierie, Sorbonne Université, UFR 933, 75005 Paris, France*

(Received 26 July 2019; accepted 9 January 2020; published 7 February 2020)

Solid-state impurity spins with optical control are currently investigated for quantum networks and repeaters. Among these, rare-earth-ion doped crystals are promising as quantum memories for light, with potentially long storage time, high multimode capacity, and high bandwidth. However, with spins there is often a tradeoff between bandwidth, which favors electronic spin, and memory time, which favors nuclear spins. Here, we present optical storage experiments using highly hybridized electron-nuclear hyperfine states in $^{171}Yb^{3+}:Y_2SiO_5$, where the hybridization can potentially offer both long storage time and high bandwidth. We reach a storage time of 1.2 ms and an optical storage bandwidth of 10 MHz that is currently only limited by the Rabi frequency of the optical control pulses. The memory efficiency in this proof-of-principle demonstration was about 3%. The experiment constitutes the first optical storage using spin states in any rare-earth ion with electronic spin. These results pave the way for rare-earth based quantum memories with high bandwidth, long storage time, and high multimode capacity, a key resource for quantum repeaters.

DOI: 10.1103/PhysRevLett.124.053606

Solid-state impurity spins play an increasingly important role in quantum information technologies, with applications in communication, computing, and sensing [1–3]. In quantum communication, solid-state spins that can be interfaced with photons are promising candidates for nodes in quantum networks and quantum repeaters. In such systems, optical transitions are used to convert quantum information between internal spin states and optical photons, where spins store and possibly process quantum information within the solid [3,4].

There is a current interest in using both the electronic and nuclear degrees of freedom of solid-state spin systems [3,5], with the goal of simultaneously achieving efficient manipulation and long-duration storage. Electronic spins couple strongly to external fields, making them ideal for high-bandwidth operations and highly sensitive sensors. The weaker coupling of the nuclear spins shields them from the environment, allowing long-duration quantum storage. However, finding spin systems that simultaneously possess good optical, electronic, and nuclear spin properties is challenging. A prominent example is the nitrogen vacancy (NV) center in diamond, where the electron spin of the NV can be coupled to photons [6], while the hyperfine interaction with neighboring ^{13}C nuclear spin provides a long-duration memory [5,7]. Similar hybrid electron-nuclear systems are investigated using ^{31}P phosphor donors in silicon [8,9] and quantum dots [10].

Rare-earth-ion (RE) doped crystals represent another prominent example of solid-state impurities with excellent optical [11] and spin properties [12]. RE crystals have emerged as strong candidates for ensemble-based quantum memories (QMs) [13–16], and more recently for single ion [17–20] quantum information processing. For ensemble-based QMs, thus far only RE nuclear spin systems have been used for storing optical pulses using spin states [21–24], based on the nuclear quadrupole states of either Pr^{3+} or Eu^{3+} ions. While these non-Kramers RE ions with quenched electronic spin provide excellent memory times, the purely nuclear states limit the memory bandwidth to < 10 MHz. RE ions with nonzero electronic spins, so-called Kramers ions, could potentially provide a solution to the bandwidth limit, provided that long coherence times can be engineered in such electronic spin systems.

Recently, it has been shown that such long spin coherence times can be found in some Kramers RE ions with electron spin $\mathbf{S}$ [25–28] and nonzero nuclear spin $\mathbf{I}$ by exploiting the hyperfine coupling $\mathbf{S}\cdot\mathbf{A}\cdot\mathbf{I}$, where $\mathbf{A}$ is the hyperfine tensor. In Refs. [27,28] it was particularly shown that at zero applied magnetic field, an anisotropic hyperfine interaction leads to strong mixing of $\mathbf{S}$ and $\mathbf{I}$, resulting in highly hybridized electron-nuclear states with zero first-order Zeeman (ZEFOZ) effect [29]. Using this feature we showed simultaneous long optical and spin coherence times of $T_2^o = 180\ \mu$s and $T_2^s = 1.5$ ms, respectively, in $^{171}Yb^{3+}:Y_2SiO_5$ [28]. We also showed that, while the hybridized states are insensitive at first order to slowly fluctuating magnetic dc fields (at the ZEFOZ point), the magnetic ac transition moment between the hybridized states remains electronic, resulting in high Rabi frequency

 © 2020 American Physical Society

and fast operations. These results are promising for broadband and long-duration optical quantum memories, but thus far there has been no demonstration of optical storage using spin states in any Kramers RE ion system.

In this Letter we demonstrate an optical memory using the hybridized electron-nuclear states at zero field in $^{171}Yb^{3+}:Y_2SiO_5$, based on the atomic frequency comb (AFC) memory scheme [30]. We reach a spin storage time of 1.2 ms and a bandwidth of 10 MHz, which is only limited by the current optical Rabi frequency. In addition, we show efficient optical AFC echoes with delays 1 order of magnitude longer than previously achieved in any Kramers system, which we attribute to reduced super-hyperfine coupling in the zero-field ZEFOZ point.

The AFC memory is based on a Δ-periodic structure of highly absorbing peaks within an inhomogeneously broadened optical transition [30]. An input pulse then produces an optical AFC echo, with a delay of $1/\Delta$. The AFC echo process allows high temporal multimode storage, provided that $1/\Delta$ is much longer than the input pulse duration [31]. To achieve on-demand read out, an optical control pulse can be applied before the AFC echo, thereby converting the optical coherence into a spin coherence. This spin-wave memory [24,32–34] is read out by applying another control pulse after a time T_S, which results in an output pulse with a storage time of $T_M = 1/\Delta + T_S$. The spin-wave storage time can be extended to the spin coherence time T_2^s by applying a spin echo sequence [34].

The memory puts specific demands on the atomic system. It requires an excited state coupled to two spin states, a so-called Λ system, where the optical memory bandwidth is ultimately limited by the spin-state energy split [30]. Efficient AFC echoes and long $1/\Delta$ delays require an optically deep and high resolution comb, which in turn requires a long optical coherence time and efficient optical pumping. Finally, long memory lifetime requires a long T_2^s and efficient spin manipulation through microwave (MW) pulses.

The optical transition we use in $^{171}Yb^{3+}:Y_2SiO_5$ connects the lowest crystal field levels in the electronic $^2F_{7/2}$ ground and $^2F_{5/2}$ excited states, at 978.854 nm (in vacuum) for site II in Y_2SiO_5 [35]. The highly anisotropic hyperfine tensors splits both levels into four nondegenerate hyperfine states at zero applied magnetic field [36], as shown in Fig. 1(a). Many different combinations of transitions could be used as the Λ system for optical storage, with corresponding microwave frequencies from 529 to 3026 MHz. Here we focus on the particular Λ system formed by the ν_1 and ν_2 transitions, see Fig. 1(a), with a spin transition at $\nu_{MW} = 655$ MHz, which has the required optical and spin coherence times [28]. A crucial first step towards optical spin-wave storage is then to demonstrate efficient optical pumping and optical AFC echoes.

Optical pumping of all hyperfine states requires addressing transitions involving all four hyperfine states. Our setup [Fig. 1(d)] is based on two lasers (master and slave), where

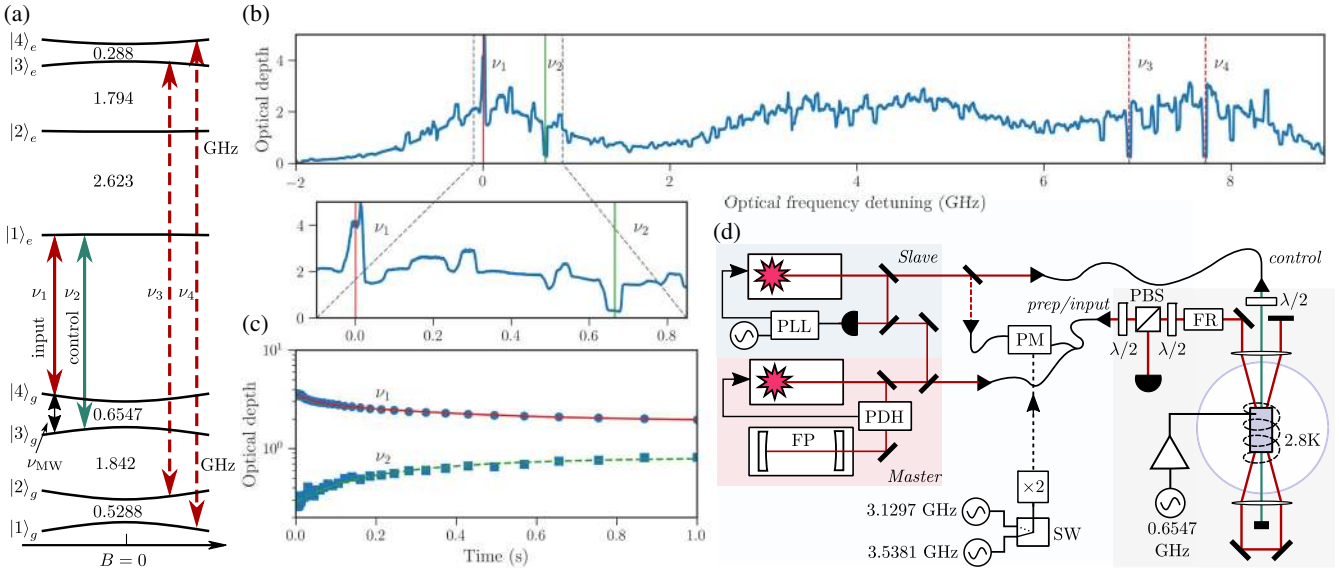

FIG. 1. Experimental setup. (a) Energy level diagram of the optical $^2F_{7/2}(0) \leftrightarrow ^2F_{5/2}(0)$ transition for site II of $^{171}Yb^{3+}:Y_2SiO_5$ crystal at zero magnetic field. The Λ system used for optical storage uses transition ν_1 for the input and output pulses and transition ν_2 for the control pulses, and ν_{MW} for the MW pulses. Transitions ν_3 and ν_4 are added for the different optical pumping steps. (b) The absorption spectrum after performing class cleaning and state initialization to the $|4\rangle_g$ ground state over a 40 MHz bandwidth. Inset: enlargement of the ν_1 and ν_2 transitions of the Λ system. (c) Optical depth of the antihole at ν_1 frequency and the hole at ν_2 frequency, as a function of delay after the state initialization. (d) Experimental setup (see text for details). Fabry-Perot cavity (FP), Pound-Drever-Hall module (PDH), phase modulator (PM), phase locked loop (PLL), half-wave plate ($\lambda/2$), polarization beam splitter (PBS), Faraday rotator (FR), microwave frequency doubler ($\times 2$), microwave switch (SW).

the master is locked to a high-finesse cavity at the frequency of the $\nu_1 = 306263.0$ GHz transition. The slave is locked to the master laser with an offset $\nu_2 = \nu_1 + 0.6547$ GHz using an optical phase lock loop (PLL). Additionally, the slave laser addresses the $\nu_3 = \nu_2 + 6.2594$ and $\nu_4 = \nu_2 + 7.0762$ GHz transitions by phase modulation [Figs. 1(a) and 1(d)].

The Y_2SiO_5 crystal is doped with 5 ppm of $^{171}Yb^{3+}$, with an isotopic purity of ≈95%. The optical inhomogeneous broadening is 1.3 GHz, hence there is clear overlap between optical transitions [Fig. 1(b)]. This issue can be solved by standard pumping sequences for RE crystals, referred to as class cleaning [37,38]. By class cleaning for 400 ms with all ν_1 to ν_4 frequencies and then state initializing into state $|4\rangle_g$ using frequencies ν_2 to ν_4, we obtain the absorption spectrum in Fig. 1(b). The strong optical absorption on the ν_1 transition and the deep holes on the ν_2 to ν_4 transitions are evidence of efficient state initialization.

A measurement of the lifetime of the absorption structure showed that it rethermalizes with two different exponential time constants [Fig. 1(c)]; a faster 36(6) ms decay and a longer 390(55) ms decay. The double decay is due to the different relaxation rates between hyperfine states, as also observed in $^{145}Nd^{3+}$ [39]. The population relaxation lifetimes are significantly longer than in the 10 ppm doped $^{171}Yb^{3+}:Y_2SiO_5$ sample used in Ref. [28], which indicates that the population relaxation is due to flip flops between ions in different hyperfine states [39–41]. A more detailed investigation of optical pumping and hyperfine flip-flop relaxation processes in this material will be presented elsewhere [42].

In a first set of storage experiments the optical AFC echo was studied (Fig. 2), without applying the optical control pulses. The AFC was created on the ν_1 transition, which has the strongest absorption in the Λ system. In particular we measured the AFC echo efficiency η_{AFC} as a function of the AFC delay $1/\Delta$, which depends strongly on the contrast and shape of the comb. The ideal shape of the comb teeth is squarish, with an optimal comb finesse given only by the maximum optical depth [43]. To create such combs we use the optical pumping method presented in Ref. [31], which was specifically designed to create optimal AFCs over a large frequency bandwidth. The AFC bandwidth was set to 20 MHz, and the 60 ms long comb preparation sequence directly followed the state initialization and class cleaning sequences.

An example of an optical AFC echo is shown in Fig. 2(a), and the echo efficiencies are plotted in Fig. 2(b). At the shortest delay of $1/\Delta = 1$ μs, the AFC echo reaches a combined storage and retrieval efficiency of $\eta_{\mathrm{AFC}} = 24\%$. The associated comb is shown in Fig. 2(c), and it features a high contrast, squarish shape that is close to optimal. The theoretical efficiency for an optimal comb for the optical depth of $d = 4$ is 32% [43]. But the experimental comb at $1/\Delta = 1$ μs has a background

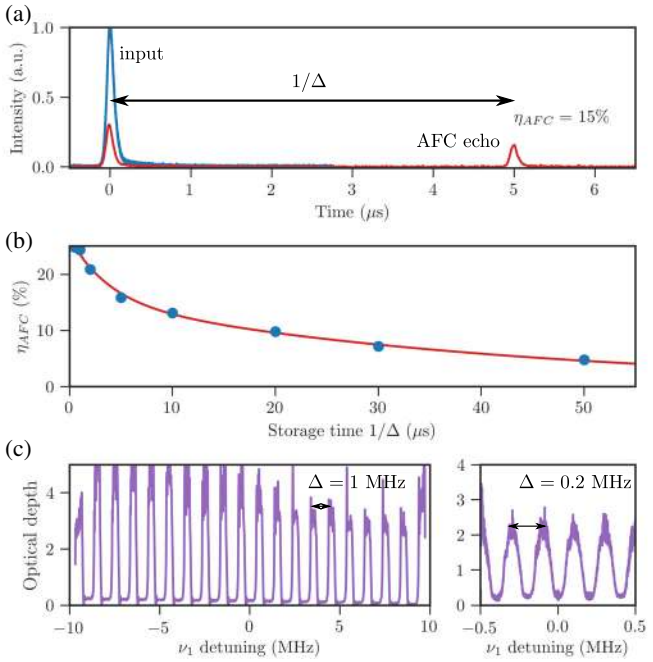

FIG. 2. Optical AFC echoes. (a) Example of an optical AFC echo for a delay of $1/\Delta = 5$ μs, with an efficiency of $\eta_{\mathrm{AFC}} = 15\%$. The input pulse duration was 100 ns. (b) AFC echo efficiencies as a function of delay $1/\Delta$ (see text for fit model). (c) Two examples of measured AFCs for $1/\Delta = 1$ and $1/\Delta = 5$ μs, in terms of optical depth d as a function of frequency detuning on the transition ν_1.

optical depth of about $d_0 \approx 0.3$, which reduces the efficiency to $0.32\exp(-d_0) = 24\%$ [44], consistent with the experimental data. Higher efficiencies should be achieved by improving the optical pumping, which requires a lower $^{171}Yb^{3+}$ concentration to reduce the flip-flop rate [40], and using optical cavities [45,46].

The decay of the AFC echo as a function of $1/\Delta$ is due to a reduction in contrast and a small deviation in shape from the optimal square one, as exemplified for $1/\Delta = 5$ μs in Fig. 2(c). The decay curve can be fitted using the formula $\exp[-4/(\Delta T_2')]$, where ideally the T_2' is the optical coherence time [31]. However, shorter T_2' are typically obtained due to technical noise such as laser coherence time limitations and cryostat vibrations. The data in Fig. 2(b) show a double exponential decay with $T_2' = 15$ and 165 μs, respectively, while the optical coherence time in this material we measured to be as long as 600 μs with photon echoes. We believe the laser spectrum to be the main limitation to the observed decay constants.

The timescale of the AFC delays shown in Fig. 2(b) is up to 2 orders of magnitude longer than previously achieved delays (0.1–1 μs) in RE ions with electronic spin degrees of freedom, such as in Nd^{3+} [14,47] or Er^{3+} [48] doped crystals. Those short decays have been explained [47,48] by invoking superhyperfine interaction between the RE electronic spin and the nuclear spin of Y^{3+} ions in the host,

which causes spectral nuclear spin-flip sidebands [49] and effectively enlarges the homogeneous linewidth of the RE ion. The efficient AFC echoes at long delays suggest that superhyperfine interaction is strongly suppressed at the zero-field ZEFOZ point. The delays are similar to those achieved in the purely nuclear RE spin systems Eu^{3+} [31] and Pr^{3+} [50], which yet again highlights the interest of the hybridization of the electronic and nuclear spins at zero field in $^{171}Yb^{3+}:Y_2SiO_5$.

We now turn to the optical spin-wave storage experiments, which in addition require coherent manipulation of the optical and microwave transitions, see Fig. 3. Optically one requires an efficient population transfer of the control pulse on the ν_2 transition, see Fig. 1(a), which has a dipole moment about 3 times weaker than the ν_1 transition (see Supplemental Material [51]). On the ν_1 transition we achieved an optical Rabi frequency of $\Omega_O = 2.0$ MHz, see Fig. 3(a), which gives an estimated Rabi frequency of $\Omega_O = 0.6$ MHz on ν_2. The resulting π-pulse duration of 0.8 μs implies an efficient population transfer over less than its Fourier limited bandwidth of 1.2 MHz, clearly insufficient for the 10 MHz bandwidth of the 100 ns input pulse. To increase the bandwidth over which efficient population transfer can be achieved, one can employ longer frequency-chirped adiabatic pulses [54]. In this case we employ hyperbolic-square-hyperbolic (HSH) pulses [55] of duration 5 μs, chirped over 10 MHz, which resulted in a measured population transfer efficiency of about 90% per HSH pulse. To reach larger memory bandwidths would require higher control pulse Rabi frequencies (see Supplemental Material [51]).

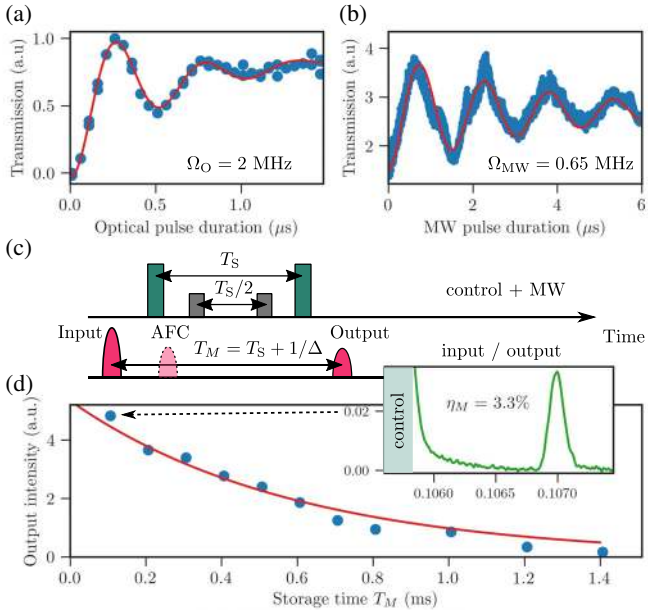

FIG. 3. AFC spin-wave storage results. (a),(b) Measured Rabi oscillations on the optical and MW transitions (see Supplemental Material [51]). (c) Pulse and timing sequence of the AFC spin-wave storage experiment, including input and output pulses (transition ν_1), control pulses (transition ν_2), and MW pulses (transition ν_{MW}). Note that for a perfect control pulse the AFC echo at $1/\Delta$ is completely suppressed. (d) The intensity of optical output pulse as a function of the total memory storage time T_M, with $1/\Delta = 7$ μs. The data were fitted to the function $\exp(-2T_S/T_2^s)$, resulting in a spin coherence time of $T_2^s = 1.2(2)$ ms. Inset: Example of output pulse trace for $T_M = 107$ μs.

On the microwave transition ν_{MW}, the stored spin coherence induced by the optical control pulse will dephase with the inverse of the inhomogeneous spin linewidth $1/\Gamma_{MW}$. We measured a spin linewidth of $\Gamma_{MW} = 0.7$ MHz (see Supplemental Material [51]), which practically makes it impossible to read out the memory given the duration of the optical control pulse. But the spin coherence can be rephased with a spin echo sequence [34,56], in this case a pair of MW π pulses greatly extends the storage time. Using a simple coil wrapped around the crystal we reached a Rabi frequency of $\Omega_{MW} = 0.65$ MHz; see Fig. 3(b). We note that with respect to pure nuclear non-Kramers systems, the spin linewidth is significantly larger. But this is more than compensated for by the electronic spin transition moment, as reflected by the large Rabi frequency. Using adiabatic MW pulses with a duration of 10 μs and a chirp bandwidth of 3 MHz, we readily reach an estimated transfer efficiency of $> 95\%$.

The final AFC spin-wave storage experiment data are shown in Fig. 3(d), as a function of the total storage time $T_M = 1/\Delta + T_S$. Memory output pulses were detectable beyond 1 ms and the memory lifetime is consistent with previous measurements of the spin coherence time in $^{171}Yb^{3+}:Y_2SiO_5$ [28]. It should be emphasized that we reach spin-wave storage times presently only achieved in $Eu^{3+}:Y_2SiO_5$ crystals using nuclear states. For the shortest spin storage time of $T_S = 100$ μs, the total memory efficiency was $\eta_M = 3.3\%$. While the AFC echo efficiency could be understood by the optical depth, see Fig. 2, the total memory efficiency falls short of our predictions by a factor of 4, given the optical and MW control pulse efficiencies given above (see Supplemental Material [51]). Possibly these were overestimated and/or their phase coherence was not sufficient.

To summarize, in this Letter we have demonstrated storage of optical pulses using the electronic-nuclear hyperfine states in $^{171}Yb^{3+}:Y_2SiO_5$, which constitutes the first demonstration of spin-wave storage in any RE ion with electronic spin. Moreover, the AFC echo delay (which is related to temporal multimode capacity) and the total spin-wave storage time reach similar performance as in the pure nuclear $^{151}Eu^{3+}:Y_2SiO_5$ system, but with 5 times larger optical bandwidths [57].

To conclude, we briefly discuss current limitations and future prospects of the memory. The memory bandwidth of 10 MHz is currently limited by the 0.6 MHz Rabi frequency of the control pulses. Simulations show (see Supplemental

Material [51]) that a 2 MHz Rabi frequency could increase the memory bandwidth to 100 MHz. Other Λ systems could reach such Rabi frequencies using different polarization modes. To efficiently excite microwave transitions at > 1 GHz in these Λ systems, one can use lumped-element MW cavities [58,59]. The optical Rabi frequency can also be greatly increased by using laser-written waveguides [50,60] and could potentially allow memory bandwidths in the range of 100 MHz to 1 GHz. This would facilitate interfacing with quantum photon pair sources [15,61], and possibly allow interfacing with quantum dot single photon sources [62–64]. There is also the prospect of greatly increasing the AFC multimode capacity, which would increase the rate of a quantum repeater [65]. By increasing the bandwidth and by achieving AFC echo delays only limited by the long optical coherence time in $^{171}Yb^{3+}:Y_2SiO_5$, the temporal multimode memory capacity could potentially reach 1000 modes. An important future step will be to demonstrate storage of weak coherent states, a strong requirement for a quantum memory. This will crucially depend on the efficiency with which one can optically pump ions out of the storage state, to decrease unwanted photon emission noise due to the control pulses. Recent work has shown that optical pumping of hyperfine states can be particularly efficient [39].

We would like to thank Antonio Ortu and Jean Etesse for fruitful discussions. We acknowledge funding from FNS Research Project No. 172590, EUs H2020 programme under the Marie Skłodowska-Curie project QCALL (GA 675662), and the ITMO Cancer AVIESAN (Cancer Plan, C16027HS, MALT).

M. B. and A. T. contributed equally to this work.

*mikael.afzelius@unige.ch
†Present address: The Niels Bohr Institute, University of Copenagen, DK-2100 Copenhagen, Denmark.
‡Present address: Department of Electrical Engineering, Princeton University, Princeton, New Jersey 08544, USA.

[1] F. Bussières, C. Clausen, A. Tiranov, B. Korzh, V. B. Verma, S. W. Nam, F. Marsili, A. Ferrier, P. Goldner, H. Herrmann, C. Silberhorn, W. Sohler, M. Afzelius, and N. Gisin, Nat. Photonics **8**, 775 (2014).
[2] C. L. Degen, F. Reinhard, and P. Cappellaro, Rev. Mod. Phys. **89**, 035002 (2017).
[3] D. D. Awschalom, R. Hanson, J. Wrachtrup, and B. B. Zhou, Nat. Photonics **12**, 516 (2018).
[4] M. Atatüre, D. Englund, N. Vamivakas, S.-Y. Lee, and J. Wrachtrup, Nat. Rev. Mater. **3**, 38 (2018).
[5] C. E. Bradley, J. Randall, M. H. Abobeih, R. C. Berrevoets, M. J. Degen, M. A. Bakker, M. Markham, D. J. Twitchen, and T. H. Taminiau, Phys. Rev. X **9**, 031045 (2019).
[6] M. W. Doherty, N. B. Manson, P. Delaney, F. Jelezko, J. Wrachtrup, and L. C. Hollenberg, Phys. Rep. **528**, 1 (2013).
[7] P. C. Maurer, G. Kucsko, C. Latta, L. Jiang, N. Y. Yao, S. D. Bennett, F. Pastawski, D. Hunger, N. Chisholm, M. Markham, D. J. Twitchen, J. I. Cirac, and M. D. Lukin, Science **336**, 1283 (2012).
[8] M. Steger, K. Saeedi, M. L. W. Thewalt, J. J. L. Morton, H. Riemann, N. V. Abrosimov, P. Becker, and H.-J. Pohl, Science **336**, 1280 (2012).
[9] K. Saeedi, S. Simmons, J. Z. Salvail, P. Dluhy, H. Riemann, N. V. Abrosimov, P. Becker, H.-J. Pohl, J. J. L. Morton, and M. L. W. Thewalt, Science **342**, 830 (2013).
[10] D. A. Gangloff, G. Éthier-Majcher, C. Lang, E. V. Denning, J. H. Bodey, D. M. Jackson, E. Clarke, M. Hugues, C. Le Gall, and M. Atatüre, Science **364**, 62 (2019).
[11] C. Thiel, T. Böttger, and R. Cone, J. Lumin. **131**, 353 (2011).
[12] M. Zhong, M. P. Hedges, R. L. Ahlefeldt, J. G. Bartholomew, S. E. Beavan, S. M. Wittig, J. J. Longdell, and M. J. Sellars, Nature (London) **517**, 177 (2015).
[13] M. P. Hedges, J. J. Longdell, Y. Li, and M. J. Sellars, Nature (London) **465**, 1052 (2010).
[14] C. Clausen, I. Usmani, F. Bussieres, N. Sangouard, M. Afzelius, H. de Riedmatten, and N. Gisin, Nature (London) **469**, 508 (2011).
[15] E. Saglamyurek, N. Sinclair, J. Jin, J. A. Slater, D. Oblak, F. Bussières, M. George, R. Ricken, W. Sohler, and W. Tittel, Nature (London) **469**, 512 (2011).
[16] Z.-Q. Zhou, W.-B. Lin, M. Yang, C.-F. Li, and G.-C. Guo, Phys. Rev. Lett. **108**, 190505 (2012).
[17] R. Kolesov, K. Xia, R. Reuter, R. Stöhr, A. Zappe, J. Meijer, P. Hemmer, and J. Wrachtrup, Nat. Commun. **3**, 1029 (2012).
[18] A. M. Dibos, M. Raha, C. M. Phenicie, and J. D. Thompson, Phys. Rev. Lett. **120**, 243601 (2018).
[19] T. Zhong, J. M. Kindem, J. G. Bartholomew, J. Rochman, I. Craiciu, V. Verma, S. W. Nam, F. Marsili, M. D. Shaw, A. D. Beyer, and A. Faraon, Phys. Rev. Lett. **121**, 183603 (2018).
[20] B. Casabone, J. Benedikter, T. Hümmer, F. Oehl, K. de Oliveira Lima, T. W. Hänsch, A. Ferrier, P. Goldner, H. de Riedmatten, and D. Hunger, New J. Phys. **20**, 095006 (2018).
[21] K. R. Ferguson, S. E. Beavan, J. J. Longdell, and M. J. Sellars, Phys. Rev. Lett. **117**, 020501 (2016).
[22] C. Laplane, P. Jobez, J. Etesse, N. Gisin, and M. Afzelius, Phys. Rev. Lett. **118**, 210501 (2017).
[23] K. Kutluer, M. Mazzera, and H. de Riedmatten, Phys. Rev. Lett. **118**, 210502 (2017).
[24] A. Seri, A. Lenhard, D. Rieländer, M. Gündoğan, P. M. Ledingham, M. Mazzera, and H. de Riedmatten, Phys. Rev. X **7**, 021028 (2017).
[25] J. M. Kindem, J. G. Bartholomew, P. J. T. Woodburn, T. Zhong, I. Craiciu, R. L. Cone, C. W. Thiel, and A. Faraon, Phys. Rev. B **98**, 024404 (2018).
[26] M. Rančić, M. P. Hedges, R. L. Ahlefeldt, and M. J. Sellars, Nat. Phys. **14**, 50 (2018).
[27] J. V. Rakonjac, Y.-H. Chen, S. P. Horvath, and J. J. Longdell, arXiv:1802.03862.
[28] A. Ortu, A. Tiranov, S. Welinski, F. Fröwis, N. Gisin, A. Ferrier, P. Goldner, and M. Afzelius, Nat. Mater. **17**, 671 (2018).
[29] E. Fraval, M. J. Sellars, and J. J. Longdell, Phys. Rev. Lett. **92**, 077601 (2004).
[30] M. Afzelius, C. Simon, H. de Riedmatten, and N. Gisin, Phys. Rev. A **79**, 052329 (2009).

[31] P. Jobez, N. Timoney, C. Laplane, J. Etesse, A. Ferrier, P. Goldner, N. Gisin, and M. Afzelius, Phys. Rev. A **93**, 032327 (2016).
[32] M. Afzelius, I. Usmani, A. Amari, B. Lauritzen, A. Walther, C. Simon, N. Sangouard, J. Minář, H. de Riedmatten, N. Gisin, and S. Kröll, Phys. Rev. Lett. **104**, 040503 (2010).
[33] M. Gündoğan, P. M. Ledingham, K. Kutluer, M. Mazzera, and H. de Riedmatten, Phys. Rev. Lett. **114**, 230501 (2015).
[34] P. Jobez, C. Laplane, N. Timoney, N. Gisin, A. Ferrier, P. Goldner, and M. Afzelius, Phys. Rev. Lett. **114**, 230502 (2015).
[35] S. Welinski, A. Ferrier, M. Afzelius, and P. Goldner, Phys. Rev. B **94**, 155116 (2016).
[36] A. Tiranov, A. Ortu, S. Welinski, A. Ferrier, P. Goldner, N. Gisin, and M. Afzelius, Phys. Rev. B **98**, 195110 (2018).
[37] L. Rippe, M. Nilsson, S. Kröll, R. Klieber, and D. Suter, Phys. Rev. A **71**, 062328 (2005).
[38] B. Lauritzen, N. Timoney, N. Gisin, M. Afzelius, H. de Riedmatten, Y. Sun, R. M. Macfarlane, and R. L. Cone, Phys. Rev. B **85**, 115111 (2012).
[39] E. Z. Cruzeiro, A. Tiranov, J. Lavoie, A. Ferrier, P. Goldner, N. Gisin, and M. Afzelius, New J. Phys. **20**, 053013 (2018).
[40] E. Z. Cruzeiro, A. Tiranov, I. Usmani, C. Laplane, J. Lavoie, A. Ferrier, P. Goldner, N. Gisin, and M. Afzelius, Phys. Rev. B **95**, 205119 (2017).
[41] B. Car, L. Veissier, A. Louchet-Chauvet, J.-L. L. Gouët, and T. Chaneliére, Phys. Rev. B **100**, 165107 (2019).
[42] S. Welinski, A. Tiranov, M. Businger, A. Ferrier, M. Afzelius, and P. Goldner, arXiv:1910.07907.
[43] M. Bonarota, J. Ruggiero, J. L. Le Gouët, and T. Chanelière, Phys. Rev. A **81**, 033803 (2010).
[44] H. de Riedmatten, M. Afzelius, M. U. Staudt, C. Simon, and N. Gisin, Nature (London) **456**, 773 (2008).
[45] M. Sabooni, Q. Li, S. Kröll, and L. Rippe, Phys. Rev. Lett. **110**, 133604 (2013).
[46] P. Jobez, I. Usmani, N. Timoney, C. Laplane, N. Gisin, and M. Afzelius, New J. Phys. **16**, 083005 (2014).
[47] I. Usmani, M. Afzelius, H. de Riedmatten, and N. Gisin, Nat. Commun. **1**, 1 (2010).
[48] I. Craiciu, M. Lei, J. Rochman, J. M. Kindem, J. G. Bartholomew, E. Miyazono, T. Zhong, N. Sinclair, and A. Faraon, Phys. Rev. Applied **12**, 024062 (2019).
[49] R. Wannemacher, R. M. Macfarlane, Y. P. Wang, D. Sox, D. Boye, and R. S. Meltzer, J. Lumin. **48–49**, 309 (1991).
[50] A. Seri, G. Corrielli, D. Lago-Rivera, A. Lenhard, H. de Riedmatten, R. Osellame, and M. Mazzera, Optica **5**, 934 (2018).
[51] See Supplemental Material at http://link.aps.org/supplemental/10.1103/PhysRevLett.124.053606 for additional experimental data, a discussion on the optical control pulse bandwidth, and a detailed experimental setup, which also includes Refs. [52,53].
[52] M. S. Silver, R. I. Joseph, and D. I. Hoult, Phys. Rev. A **31**, 2753 (1985).
[53] J. Appel, A. MacRae, and A. I. Lvovsky, Meas. Sci. Technol. **20**, 055302 (2009).
[54] J. Minář, N. Sangouard, M. Afzelius, H. de Riedmatten, and N. Gisin, Phys. Rev. A **82**, 042309 (2010).
[55] M. Tian, T. Chang, K. D. Merkel, and W. R. Babbitt, Appl. Opt. **50**, 6548 (2011).
[56] G. Heinze, C. Hubrich, and T. Halfmann, Phys. Rev. Lett. **111**, 033601 (2013).
[57] C. Laplane, P. Jobez, J. Etesse, N. Timoney, N. Gisin, and M. Afzelius, New J. Phys. **18**, 013006 (2016).
[58] Y.-H. Chen, X. Fernandez-Gonzalvo, and J. J. Longdell, Phys. Rev. B **94**, 075117 (2016).
[59] A. Angerer, T. Astner, D. Wirtitsch, H. Sumiya, S. Onoda, J. Isoya, S. Putz, and J. Majer, Appl. Phys. Lett. **109**, 033508 (2016).
[60] G. Corrielli, A. Seri, M. Mazzera, R. Osellame, and H. de Riedmatten, Phys. Rev. Applied **5**, 054013 (2016).
[61] C. Clausen, F. Bussières, A. Tiranov, H. Herrmann, C. Silberhorn, W. Sohler, M. Afzelius, and N. Gisin, New J. Phys. **16**, 093058 (2014).
[62] T. Grange, N. Somaschi, C. Antón, L. De Santis, G. Coppola, V. Giesz, A. Lemaître, I. Sagnes, A. Auffèves, and P. Senellart, Phys. Rev. Lett. **118**, 253602 (2017).
[63] G. Kiršanskė, H. Thyrrestrup, R. S. Daveau, C. L. Dreeßen, T. Pregnolato, L. Midolo, P. Tighineanu, A. Javadi, S. Stobbe, R. Schott, A. Ludwig, A. D. Wieck, S. I. Park, J. D. Song, A. V. Kuhlmann, I. Söllner, M. C. Löbl, R. J. Warburton, and P. Lodahl, Phys. Rev. B **96**, 165306 (2017).
[64] L. Schweickert, K. D. Jöns, K. D. Zeuner, S. F. C. da Silva, H. Huang, T. Lettner, M. Reindl, J. Zichi, R. Trotta, A. Rastelli, and V. Zwiller, Appl. Phys. Lett. **112**, 093106 (2018).
[65] C. Simon, H. de Riedmatten, M. Afzelius, N. Sangouard, H. Zbinden, and N. Gisin, Phys. Rev. Lett. **98**, 190503 (2007).